

# Rapid Preparation Method for Preparing Tracheal Decellularized Scaffolds: Vacuum Assistance and Optimization of DNase I

Zhihao Wang,<sup>†</sup> Fei Sun,<sup>†</sup> Yi Lu, Boyou Zhang, Guozhong Zhang, and Hongcan Shi\*



Cite This: *ACS Omega* 2021, 6, 10637–10644



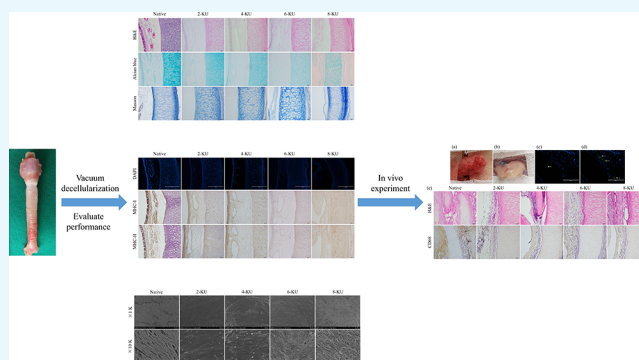
Read Online

ACCESS |

Metrics & More

Article Recommendations

**ABSTRACT:** Decellularized scaffolds are an effective way for tracheal tissue engineering to perform alternative treatments. However, clinically used decellularized tracheal scaffolds have a long preparation cycle. The purpose of this study is to improve the efficiency of decellularization by vacuum assistance and optimizing the concentration of DNase I in the decellularization process and to quickly obtain tracheal decellularized scaffolds. The trachea of New Zealand white rabbits was decellularized with 2, 4, 6, and 8 KU/mL DNase I under vacuum. The performance of the decellularized tracheal scaffold was evaluated through histological analysis, immunohistochemical staining, DNA residue, extracellular matrix composition, scanning electron microscopy, mechanical properties, cell compatibility, and *in vivo* experiments. Histological analysis and immunohistochemical staining showed that compared with the native trachea, the hierarchical structure of the decellularized trachea remained unchanged after decellularization, nonchondrocytes were effectively removed, and the antigenicity of the scaffold was significantly weakened. Deoxyribonucleic acid (DNA) quantitative analysis showed that the amount of residual DNA in the 6-KU group was significantly decreased. Scanning electron microscopy and mechanical tests showed that small gaps appeared in the basement membrane of the 6-KU group, and the mechanical properties decreased. The CCK-8 test results and *in vivo* experiments showed that the 6-KU group's acellular scaffold had good cell compatibility and new blood vessels were visible on the surface. Taken together, the 6-KU group could quickly prepare rabbit tracheal scaffolds with good decellularization effects in only 2 days, which significantly shortened the preparation cycle reducing the required cost.



## 1. INTRODUCTION

In clinical practice, the trachea is often damaged by stenosis, tumors, trauma, infection, and other factors. When the length of the injury is less than 1/2 of the full length of an adult or 1/3 of a child, surgical removal and end-to-end anastomosis are the “gold standard of treatment”.<sup>1–5</sup> However, when tracheal injury exceeds this length, conventional endoscopic or open surgery cannot meet the needs of the condition, and further tracheal replacement therapy is needed.<sup>6–8</sup> Tissue engineering scaffolds composed of decellularized scaffolds, synthetic scaffolds, and composite scaffolds provide a new method for airway reconstruction.<sup>9–14</sup> The ideal tracheal scaffold should retain the main structure, extracellular matrix (ECM), airtightness, and mechanical properties of the trachea, which are similar to the normal tracheal structure and function. Additionally, it removes immunogenicity and reduces complications such as the immune response and rejection after transplantation.<sup>3,15</sup> By decellularizing the donor trachea, the anatomical structure and function of the trachea can be preserved while removing the core components of the scaffold, which is an effective method for tracheal tissue engineering in tracheal replacement therapy.<sup>16–18</sup>

At present, decellularized tracheal scaffolds prepared using a detergent combined with the enzymatic method (DEM) have been used in clinical cases and have shown better results, but the preparation of decellularized tracheal matrices takes several weeks to several months.<sup>19,20</sup> Their long preparation time cannot be conducive for patients with acute tracheal diseases that require rapid tracheal replacement therapy in clinical practice, such as tracheal hypoplasia and atresia.<sup>21,22</sup> The clinicalization of tracheal tissue engineering requires not only the good characteristics of tracheal scaffolds but also a suitable production cycle. By shortening the preparation time of the scaffold, the production cost and time cost can be reduced, and the clinical application prospect of the tracheal scaffold can be improved.

Received: December 23, 2020

Accepted: March 3, 2021

Published: April 16, 2021



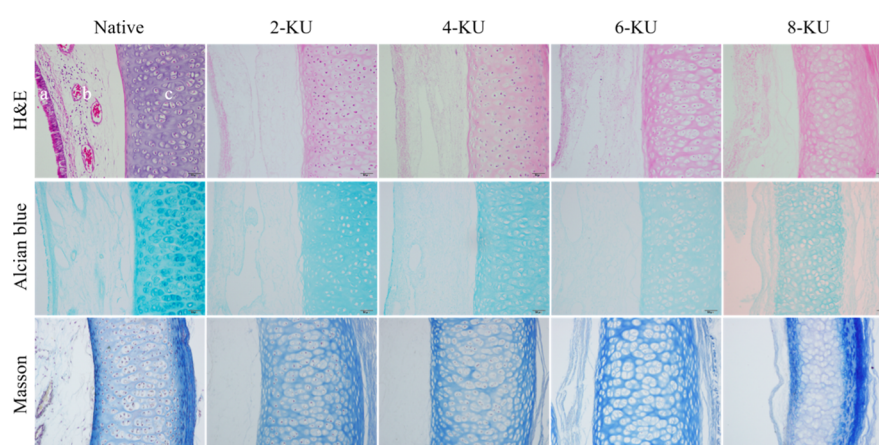


**Figure 1.** Structural changes of the scaffold before and after tracheal decellularization (a–d refer to the mucosa, submucosa, cartilage, and adventitia of the trachea, respectively).

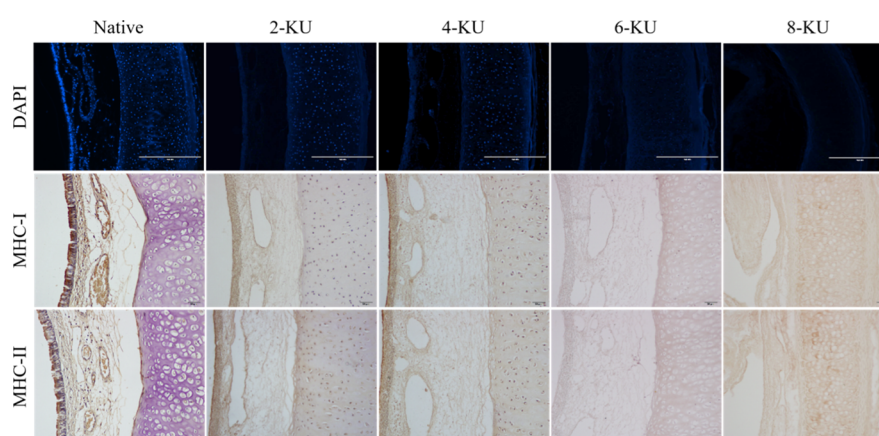


**Figure 2.** Evaluation of the decellularization effect.

Therefore, this experiment explored a strategy to quickly obtain decellularized tracheal scaffolds. Through the vacuum negative pressure state and optimizing the concentration of DNase I in the decellularization process, the entry of detergents and enzymes into the tissue is accelerated, and the effect and efficiency of decellularization are improved, thereby significantly reducing the time for preparing tracheal decellularized scaffolds.<sup>23,24</sup> The optimal concentration of DNase I for rapid preparation of tracheal decellularized scaffolds under vacuum was screened out through comprehensive comparison of deoxyribonucleic acid (DNA) residues in the scaffold, changes in the ECM components, mechanical properties, and cell compatibility, and in vivo experiments. This study aims to reduce the preparation time of decellularized tracheal scaffolds and reduce the cost of scaffold preparation.

## 2. RESULTS AND DISCUSSION

**2.1. Histological Analysis.** After vacuum decellularization treatment, the changes in the ECM of the scaffold were evaluated by hematoxylin and eosin (H&E), Masson's trichrome, and Alcian Blue staining, and the results are shown in Figure 1. H&E staining showed that the mucosal layer of the native tracheae had tightly ordered cilia, and there were also a large number of scattered cell nuclei in the submucosa, cartilage, and adventitia. After decellularization, cilia on the luminal surface of the trachea disappear, and the

nuclei of noncartilage structures such as the luminal epithelium (mucosa), submucosa, and adventitia are basically removed. With increasing DNase I treatment concentration, the cartilage nucleus was gradually removed. When the DNase I concentration was 8 KU/mL, the cartilage nucleus was almost completely removed. Masson tricolor showed that compared with the native group, there was no significant change in the collagen fiber content in the tracheal scaffolds in each group after vacuum decellularization. Alcian blue staining was used to evaluate glycosaminoglycans (GAG) in the ECM. The staining showed that the GAG in the matrix was defective after decellularization. With increasing DNase I concentration, the GAG defect further expanded; the GAG content loss in the ECM of the 8-KU group was the greatest and the coloring was the lightest.

**2.2. Efficacy of Tracheal Decellularization.** 4'-6-Diamidino-2-phenylindole (DAPI) staining showed dense blue fluorescence on the tracheal mucosa of the native control group, indicating that there are a large number of highly concentrated DNA fragments in the mucosal epithelium, and a large amount of blue fluorescence is also scattered in the submucosa, cartilage, and adventitia, as shown in Figure 2. After decellularization, the nuclei of the tracheal mucosa, submucosa, and adventitia were almost completely removed, and no obvious fluorescent staining was seen, while more residual DNA fluorescent staining was still seen in the cartilage. With increasing DNase I concentration, the intensity of the

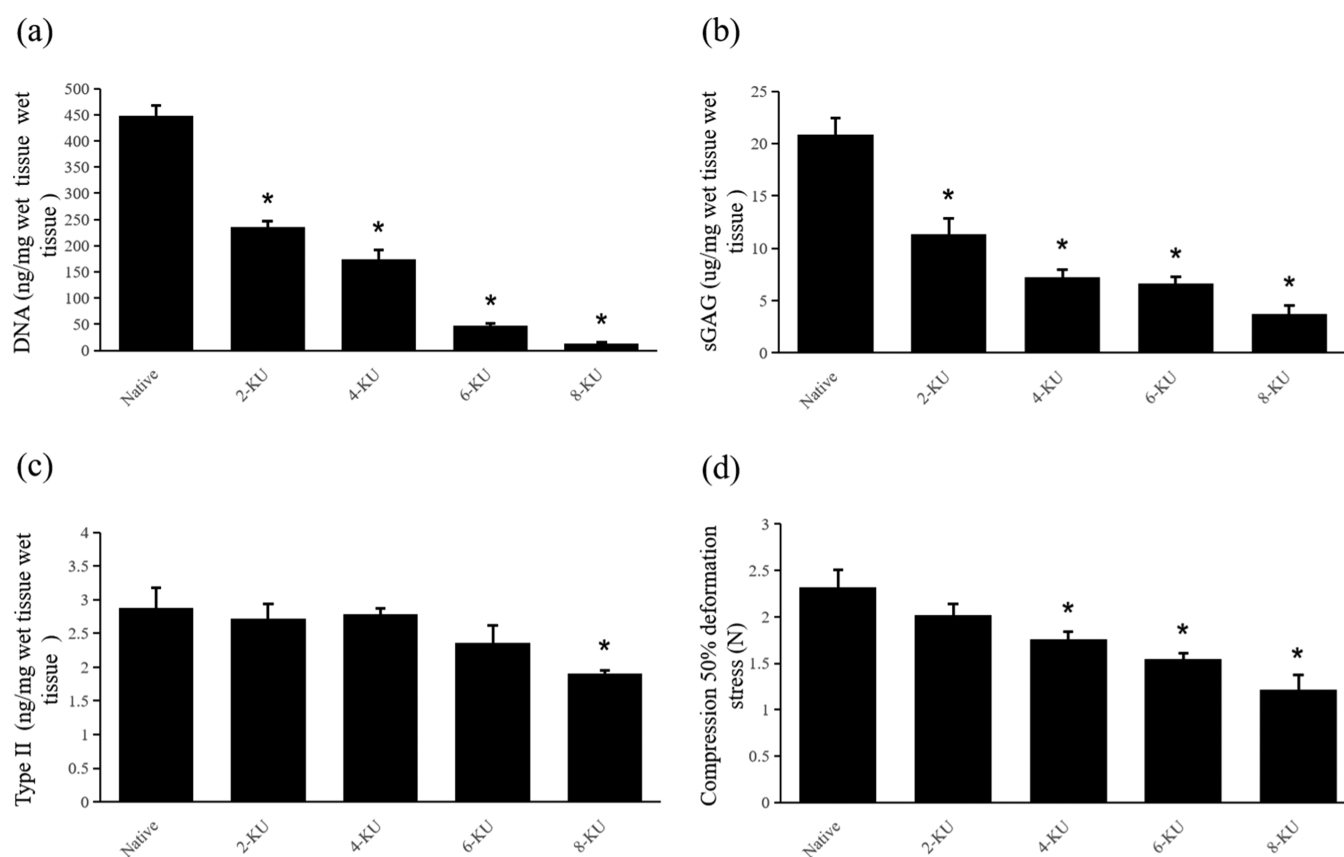


**Figure 3.** Changes in the composition and mechanical properties of the ECM of the scaffold (\* compared with the native tracheae,  $p < 0.05$ ). (a) Quantitative analysis of residual DNA in each group of tracheal scaffolds. (b,c) Quantitative analyses of type II collagen and sGAG, respectively. (d) Load when the scaffolds is compressed to 50% of the starting diameter.

fluorescence signal gradually weakened. The fluorescence signal of the 6-KU group was dim, indicating that the residual amount of DNA was significantly reduced. The blue fluorescence signal in the cartilage area of the 8-KU group basically disappeared, and the DNA in the cartilage circle was almost completely removed.

To further evaluate the effect of decellularization, DNA quantitative analysis was performed, and the results are shown in Figure 3A. Compared with the native tracheae ( $450 \pm 20$  ng/mg), the residual DNA content in the scaffold in the 6-KU group ( $50 \pm 5$  ng/mg,  $p < 0.05$ ) decreased significantly, and the residual DNA content in the 8-KU group ( $15 \pm 10$  ng/mg,  $p < 0.05$ ) further decreased.

Immunohistochemical staining further evaluated the immunogenicity of the tracheal scaffold after decellularization. The results showed that the expression of MHC-I and MHC-II in the native tracheae was strongly positive and was mainly distributed in the epithelial cells of the tracheal mucosa. After decellularization, the positive expression of MHC-I and MHC-II in the scaffold was significantly reduced, as shown in Figure 2.

**2.3. ECM Quantification.** Quantitative analysis of sulfated glycosaminoglycans (sGAG) showed that the sGAG content was greatly depleted after vacuum decellularization, as shown in Figure 3B. Compared with the native tracheae ( $20.82 \pm 1.63$   $\mu\text{g}/\text{mg}$ ), the sGAG content of the 6-KU group ( $6.62 \pm 0.66$   $\mu\text{g}/\text{mg}$ ,  $p < 0.05$ ) decreased significantly. With the increase in the DNase I concentration during the decellularization process,

the sGAG content of the 8-KU group ( $3.72 \pm 0.85$   $\mu\text{g}/\text{mg}$ ) was further lost.

The quantitative analysis results of type II collagen are shown in Figure 3C. Compared with the native tracheae ( $2.67 \pm 1.15$  ng/mg), the content of type II collagen in the 2-KU group, 4-KU group, and 6-KU group ( $2.61 \pm 0.85$ ,  $2.64 \pm 0.34$ , and  $2.45 \pm 0.65$  ng/mg,  $p > 0.05$ ) did not change significantly, while the content of type II collagen in the 8-KU group ( $2.23 \pm 0.18$  ng/mg,  $p < 0.05$ ) had a certain loss, similar to the decellularization effect of DEM.<sup>25,26</sup>

**2.4. Biomechanical Properties.** The maintenance of the mechanical properties of the scaffold is an important index for the transplantation of tracheal tissue engineering in vivo. To evaluate whether the vacuum decellularization process damages the mechanical properties of the scaffold, the scaffolds treated with different DNase I concentrations were compared with the control trachea. The results showed that the anticompression performance of the rabbit trachea was weakened after vacuum decellularization. The 50% compression deformation stress (N) gradually decreased with increasing DNase I concentration, and the 50% compression deformation stress of the 6-KU DNase I group was only 72% of the native tracheae, and the further decrease in the 8KU group was only 52% of the natural trachea, as shown in Figure 3D. After compression, each group of tracheal scaffolds returned to a similar shape before the test.

**2.5. Scanning Electron Microscopy.** A scanning electron microscope was used to observe the three-dimensional structure of the trachea and ECM microstructure before and

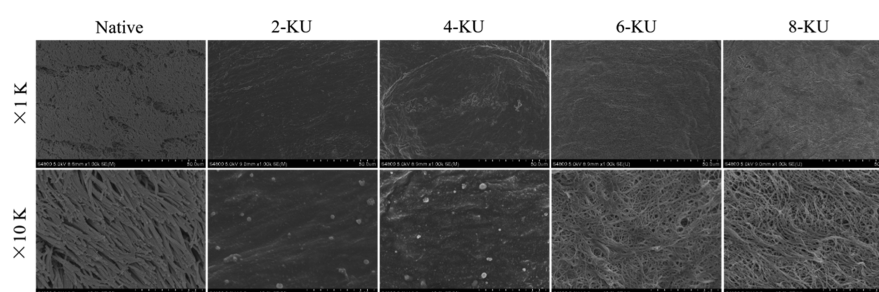


**Figure 4.** SEM image of the inner surface of the decellularized scaffold.

**Table 1.** Cytocompatibility of Scaffolds after Decellularization with Different DNase I Concentrations (OD Value)

	native	2-KU	4-KU	6-KU	8-KU
1d	0.126 ± 0.006	0.142 ± 0.009	0.149 ± 0.015	0.161 ± 0.019 <sup>a</sup>	0.228 ± 0.058 <sup>a</sup>
3d	0.158 ± 0.012	0.182 ± 0.020	0.199 ± 0.025	0.228 ± 0.033 <sup>a</sup>	0.312 ± 0.067 <sup>a</sup>
5d	0.178 ± 0.010	0.216 ± 0.012	0.245 ± 0.057 <sup>a</sup>	0.378 ± 0.023 <sup>a</sup>	0.461 ± 0.029 <sup>a</sup>
7d	0.206 ± 0.015	0.289 ± 0.032 <sup>a</sup>	0.338 ± 0.048 <sup>a</sup>	0.469 ± 0.021 <sup>a</sup>	0.608 ± 0.043 <sup>a</sup>

<sup>a</sup>ANOVA:  $p < 0.05$  compared with the native tracheae.

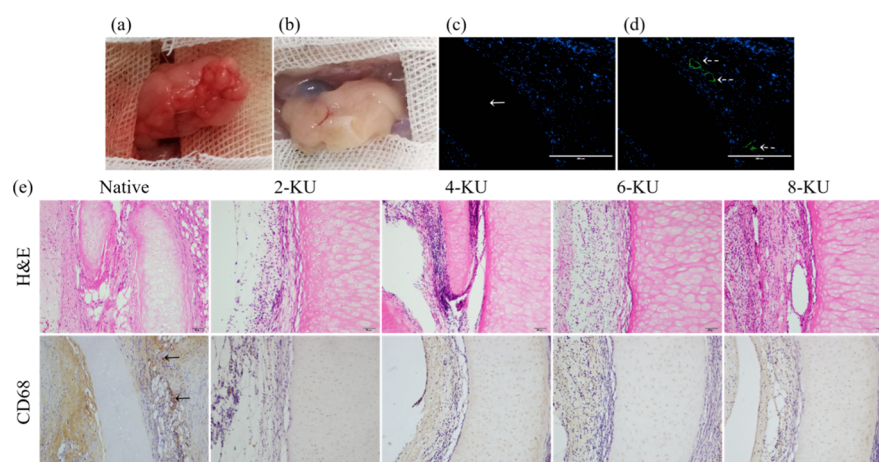


**Figure 5.** In vivo biocompatibility of decellularized scaffolds. (a) Scaffold is embedded in the greater omentum of the rat. (b) Harvesting of the postoperative graft. (c) DAPI staining in the postoperative 6KU group. (d) Immunofluorescence staining of CD31 in the postoperative 6KU group. (e) H&E and CD68 staining of the scaffolds in each postoperative groups.

after decellularization. It can be seen under the microscope that there are a large number of cilia on the lumen surface of the native tracheae, and the swing is consistent. The cilia on the matrix lumen surface of the 2-KU, 4-KU, 6-KU, and 8-KU groups were all removed, as shown in Figure 4. After vacuum decellularization treatment, each group of the acellular matrix retains the hierarchical structure of the tissue, and the matrix basement membrane is relatively complete. However, as the concentration of DNase I increased during the decellularization process, the basement membrane of the 6-KU group showed more small gaps, collagen fibers were exposed, the basement membrane cracks of the 8-KU group were further enlarged, and the structure was loose, as shown in Figure 4.

**2.6. Cell Compatibility of Decellularized Trachea.** The biocompatibility of the scaffold is also an important indicator of transplantation in vivo. The cell biocompatibility of the scaffold was preliminarily evaluated through an in vitro cell proliferation test. Bone marrow mesenchymal stem cells (BMSCs) have a variety of differentiation potential, are easy to separate, purify, and proliferate, and are an important source of seed cells for tissue engineering.<sup>27,28</sup> BMSCs were inoculated on the inner surface of the scaffold for the in

vitro cell proliferation test. The CCK-8 test results showed that the number of cells in each group continued to increase during the first 7 days. Analyzing the OD value of each group, it can be seen that compared with the native tracheae, the number of cells in the 6-KU group and the 8-KU group was significantly increased, indicating that the biocompatibility of the tracheal matrix increased after vacuum decellularization treatment, supporting cell adhesion, growth, and proliferation on its surface, as shown in Table 1.

**2.7. In Vivo Experiment.** To further evaluate the biocompatibility of the scaffold treated with different DNase I concentrations under vacuum, the scaffold was embedded in the omentum of SD rats (Figure 5A) and removed 30 days after the operation. During the experiment, the rats behaved normally, with no adverse reactions and no signs of death or implant discharge. Thirty days later, the graft was removed from the omentum of the recipient. The surface of the decellularized tracheal scaffold was visually attached with new blood vessels, the surface was smooth, and the tissue infiltrated from the recipient around the graft without purulent infection (Figure 5B). Postoperative H&E staining showed that the native tracheae and each decellularized group had similar

neutrophil responses around the tracheal grafts. The cartilage area of the 6-KU group had no host cell penetration and was completely decellularized (Figure 5E). DAPI staining also confirmed that there was no DNA residue in the cartilage (Figure 5C).

The results of CD31 immunofluorescence staining showed that 30 days after the graft was embedded in the omentum, the surface of the scaffold in the 6-KU group showed obvious neovascular infiltration, and the biocompatibility was good (Figure 5D). CD68 staining showed that the CD68 staining of each decellularized group was negative, and there was almost no macrophage infiltration. However, in the native tracheae, more macrophage infiltration was seen in the native trachea, and the rejection reaction was severe (Figure 5E).

The ideal decellularization program can almost or completely remove the cellular material that can cause the immune response, retain the ECM structure, facilitate good biocompatibility, and can be used as a biological scaffold for tissue engineering regeneration therapy.<sup>29–32</sup> By comparing the decellularization efficiency, ECM changes, cell compatibility, mechanical properties, and in vivo responses of tracheal scaffolds treated with different DNase I concentrations under vacuum, this study proved that vacuum assistance and optimization of DNase I can accelerate the process of tracheal decellularization and reduce the preparation cycle and production costs. In this program, it only takes 2 days from the initial acquisition of the rabbit trachea to the preparation of the scaffold. In contrast, the DEM method requires more than 9 days.<sup>25,33</sup>

Complete decellularization is necessary to reduce immune and inflammatory responses, but the efficiency of decellularization methods or programs depends on the structure and density of the target tissue.<sup>34</sup> The tracheal cartilage structure is dense, making it difficult for detergents and enzymes to penetrate. Under the premise of ensuring the decellularization effect and without adding chemical reagents, this study used vacuum negative pressure technology and increased the concentration of DNase I during the decellularization process to speed up the efficiency of detergents and enzymes entering the tracheal tissue, improve the decellularization effect, and shorten the preparation cycle of acellular scaffolds.<sup>23,24,26</sup> DAPI staining of the 6-KU DNase I group showed that the DNA in tracheal cartilage was almost completely removed after decellularization, and the average amount of residual DNA per mg wet weight of ECM was 50 ng dsDNA. DAPI staining in the 8-KU DNase I group showed no fluorescence signal in the cartilage circle, and the average residual amount of DNA per mg ECM was only 15 ng dsDNA. The clinical application standard of the DNA content in decellularized scaffolds is 50 ng/mg of residual DNA in tissues.<sup>31,35</sup> Compared with the natural trachea, the 2KU group and the 4KU group, the DNA residues in the 6KU DNase I group and the 8KU DNase I group all reached this standard. Moreover, this study further accelerated the process of decellularization. It only takes 2 days from the trachea to complete the decellularization. It only takes 2 days from tracheal acquisition to completion of decellularization. These results prove that the vacuum-assisted method is faster than the decellularization under normal pressure, and the decellularization effect after DNase I concentration optimization is more thorough than the conventional DEM treatment. Although the decellularization effect of this research program has reached the ideal state and shortened the decellularization cycle, the mechanical properties of the tracheal decellularized

scaffold have not been fully preserved. Biomechanical experiments showed that the mechanical properties of the decellularized scaffold gradually weakened as the concentration of DNase I increased. The 50% compression deformation stress of the 6-KU DNase I group was only 72% of the native tracheae, and the further decrease in the 8KU group was only 52% of the natural trachea. The weakening of the mechanical properties of acellular scaffolds may be related to the loss of GAG during the decellularization process, as in other studies.<sup>36,37</sup>

Good biocompatibility is a key indicator for scaffold transplantation in vivo.<sup>38,39</sup> Clinically, autologous cells are often used for scaffold reconstruction, such as epithelial cells, mesenchymal stromal cells (MSCs), and MSC-derived chondrocytes.<sup>20,40–42</sup> In this study, BMSCs were seeded on the inner surface of the acellular scaffold to explore the cell biocompatibility of the scaffold. The CCK-8 test results showed that the acellular scaffold supports the adhesion and proliferation of BMSCs. CD68 immunohistochemical staining also confirmed that after vacuum DNase I decellularization, the immunogenicity of the decellularized scaffold was effectively removed. The scaffold has good biocompatibility in vivo, and no macrophage expression is seen in each group of the decellularized scaffolds.

The vascularization of tracheal scaffolds has always been a major problem in tracheal replacement therapy. Its mechanism, process, and effects are currently unclear, and further research is needed.<sup>43–45</sup> In this study, the decellularized scaffold was embedded in the allogeneic omentum, and the decellularized rabbit tracheal scaffold was removed from the rat omentum 30 days later. In the 6-KU DNase I group, new blood vessels were visible on the surface of the scaffold, and CD31 staining further confirmed that there was neovascular infiltration in the scaffold. In vivo experiments further show that the decellularized scaffold prepared in this study supports angiogenesis and has good biocompatibility. In the clinic, human tube donors are very scarce, and xenotransplantation can provide an effective solution to this problem. Through the exploration of the heterologous omentum-embedding experiment of the decellularized tracheal scaffold, this study provided data-based support for solving the problem of clinical tracheal donor shortages in the future.

### 3. CONCLUSIONS

In summary, this study explored a method for rapidly preparing rabbit acellular tracheal scaffolds. By comprehensively comparing the performance of each group of tracheal decellularized scaffolds, it was found that the 6-KU group can be used to quickly prepare rabbit tracheal scaffolds with good decellularization effects in only 2 days, which significantly shortens the preparation cycle and reduces costs. This research provides new ideas for emergency replacement therapy for the trachea and other organs.

### 4. EXPERIMENTAL SECTION

**4.1. Materials.** Male New Zealand white rabbits weighing  $2.5 \pm 0.5$  kg ( $n = 30$ ) were selected and purchased from the Experimental Animal Center of Clinical Medicine of Yangzhou University (Yangzhou, China), license number: SYXK2016-0019. All animals were treated for humanitarian care in accordance with the “Guidelines for Ethical Review of Laboratory Animal Welfare” formulated by the Ministry of

Science and Technology and complied with the requirements of the Ethics Committee of Yangzhou University Medical School.

Using random arithmetic, 30 New Zealand white rabbits were divided into five groups. Group A ( $n = 6$ ): the native control group (native tracheae); group B ( $n = 6$ ): the 2-KU DNase I group; group C ( $n = 6$ ): the 4-KU DNase I group; group D ( $n = 6$ ): the 6-KU DNase I group; and group E ( $n = 6$ ): the 8-KU DNase I group.

**4.2. Preparation of the Tracheal Scaffold.** The New Zealand rabbits in each group were sacrificed by air embolism in the marginal ear vein, and the trachea was obtained by rapidly separating the tissue under the principle of asepticity. The obtained natural trachea is soaked in 4 °C phosphate-buffered saline (PBS) containing 1% antibiotics and anti-bacterial drugs (AA) to clean, and the residual tissue on the trachea was removed and then decellularized. The following decellularization process is carried out under vacuum conditions. A disposable vacuum blood collection tube (without substrate) is used as a container for holding different buffers for decellularization. The container is evacuated to 1/2 standard atmospheric pressure (50.66 kPa) after each buffer change using a vacuum pump equipped with a display. First, the experimental group was infiltrated and dissolved in sterile-distilled water at 4 °C for 24 h, incubated in 4% sodium deoxycholate solution (Sigma) for 4 h, and washed with PBS three times (10 min/wash). Then, the samples were immersed in 1 mol/L NaCl solution containing 2, 4, 6, and 8 KU/mL DNase I (Sigma) and incubated at 37 °C in a shaker for 12 h (100 rpm). The decellularized tissue was transferred to the PBS solution and sonicated for 30 min at room temperature, followed by PBS washing three times (10 min/wash) to remove tissue fragments. Finally, the sample was stored in 4 °C PBS buffer containing 1% AA for testing.

**4.3. Histological Staining.** The samples were fixed with 10% neutral formaldehyde (pH 7.4) for 24 h at room temperature, embedded in paraffin, and sectioned (4  $\mu$ m). To explore the structural changes of the decellularized scaffolds, H&E (Beyotime), Masson tricolor (Leagene), and Alcian blue staining (Solarbio) were performed, and the tissue morphological changes were observed under an optical microscope (Olympus).

**4.4. Evaluation of the Decellularization Effect.** DAPI can bind to double-stranded DNA and emit strong blue fluorescence. The changes in blue fluorescence after DAPI staining between groups were observed using a fluorescence microscope to evaluate the removal of nuclear components after tracheal decellularization. The tracheal scaffolds in each group were quantitatively analyzed for DNA residues. The DNA was extracted according to the operation steps of the tissue genomic DNA extraction kit (Solarbio), and the eluted DNA was quantified using a microplate reader (BioTeK, Thermo). The 260/280 ratio of all samples is between 1.8 and 2.0.

The presence of the major histocompatibility complex (MHC) in the tracheal scaffold was detected by immunohistochemistry to evaluate the effect of the decellularization program. In short, the primary antibody (MHC-I or MHC-II, dilution 1:200, Bio-Rad) is incubated overnight at 4 °C, followed by the secondary antibody (goat antirabbit/mouse IgG, MXB) forming an immune complex with the primary antibody on the tissue, then Streptomyces' antibiotin protein–peroxidase is added to link with the immune complex, and

finally 3,3'-diaminobenzidine is reacted with peroxidase to stain the antigenic site bound by the primary antibody in the tissue section. The images were taken using cellSens Entry to compare the expression levels of MHC-I and MHC-II antigens in each group of the samples.

**4.5. Quantitative Analysis of GAGs and Type II Collagen.** Quantitative analysis of sGAG was carried out with the GAG assay kit (Biocolor). The same amount of samples from each group was soaked in 1 mL papain extract and incubated at 65 °C for 18 h. The dye reagent and sGAG combine to form a particulate complex, which is then dissolved by adding a dissociation reagent. Then, 200  $\mu$ L of the solution is taken to measure the absorbance at 656 nm, and the sGAG concentration is obtained according to the standard curve.

The rabbit type II collagen ELISA kit (Bioswamp) was used to quantify the type II collagen content in the samples, and the wet weight of each group of samples was weighed. After homogenization, the supernatant was extracted, and the type II collagen content was determined. The supernatant is combined with HRP-labelled type II collagen antibody to form an antibody–antigen–enzyme-labelled antibody complex, which is washed thoroughly and then added to the substrate TMB for color development. A microplate reader was used to detect the absorbance at 450 nm and calculate the concentration according to the standard curve of the rabbit type II glue.

**4.6. Scanning Electron Microscope Observation.** The surface morphology of the tracheal decellularized scaffold was observed using a scanning electron microscope (S-4800, Hitachi). The sample was fixed with 2.5% glutaraldehyde for 24 h, dehydrated with gradient ethanol, and dried at the critical point of CO<sub>2</sub>. After spraying gold, the scaffold was observed and analyzed with a scanning electron microscope.

**4.7. Biomechanics Test.** The mechanical properties of each group of brackets are tested using a universal testing machine (AGS-X-10Kn, Shimadzu). The scaffold was compressed along the transverse axis of the scaffold at a constant rate of 3 mm/min at room temperature. The load ( $N$ ) exerted by the scaffold was calculated when the scaffold was compressed to 50% of the starting diameter.

**4.8. Cell Compatibility of the Scaffold.** According to our research team's previous BMSC culture program,<sup>28</sup> BMSCs cultured to the fourth generation were implanted in each group of tracheas of 0.5 cm  $\times$  0.5 cm<sup>2</sup> with a cell density of  $0.5 \times 10^4$ /well. The OD value was measured using the CCK-8 method (Biosharp) on days 1, 3, 5, and 7 to evaluate the proliferation and attachment status of the cells on the scaffold.

**4.9. In Vivo Biocompatibility.** In vivo experiments further explored the biocompatibility of tracheal decellularized scaffolds. The scaffolds of each group were embedded in the omentum of adult male SD rats, and the grafts were removed for histopathological analysis 30 days later. H&E staining was used to observe the postoperative changes in the tracheal structure. CD68 immunohistochemical staining (1:200 dilution, Abcam) was used to mark the expression of macrophages in the decellularized scaffold, and CD31 immunofluorescence staining (1:200 dilution, Bioss) was used to evaluate the vascularization ability of the decellularized scaffold after transplantation.

**4.10. Statistical Analysis.** SPSS 19.0 statistical software was used for data analysis, and the data of each group are expressed as the mean  $\pm$  standard deviation (mean  $\pm$  SD). The comparison between the two groups was performed using

the *t*-test, the analysis of variance was used for three groups and above, and the difference was statistically significant if  $p < 0.05$ .

## AUTHOR INFORMATION

### Corresponding Author

**Hongcan Shi** – Department of Thoracic Surgery, School of Clinical Medicine, Yangzhou University, and Center for Translational Medicine Research, Yangzhou University, Yangzhou 225000, China; Email: [shihongcan@yzu.edu.cn](mailto:shihongcan@yzu.edu.cn)

### Authors

**Zhihao Wang** – Department of Thoracic Surgery, School of Clinical Medicine, Yangzhou University, and Center for Translational Medicine Research, Yangzhou University, Yangzhou 225000, China; [orcid.org/0000-0002-4808-9644](https://orcid.org/0000-0002-4808-9644)

**Fei Sun** – Department of Thoracic Surgery, School of Clinical Medicine, Yangzhou University, and Center for Translational Medicine Research, Yangzhou University, Yangzhou 225000, China

**Yi Lu** – Department of Thoracic Surgery, School of Clinical Medicine, Yangzhou University, and Center for Translational Medicine Research, Yangzhou University, Yangzhou 225000, China

**Boyong Zhang** – Department of Thoracic Surgery, School of Clinical Medicine, Yangzhou University, and Center for Translational Medicine Research, Yangzhou University, Yangzhou 225000, China

**Guozhong Zhang** – Department of Thoracic Surgery, School of Clinical Medicine, Yangzhou University, and Center for Translational Medicine Research, Yangzhou University, Yangzhou 225000, China

Complete contact information is available at:

<https://pubs.acs.org/10.1021/acsomega.0c06247>

### Author Contributions

<sup>†</sup>Z.W. and F.S. contributed equally to this work.

### Notes

The authors declare no competing financial interest.

## ACKNOWLEDGMENTS

This research was supported by the National Natural Science Foundation of China (grant nos 81770018 and 82070020) and Jiangsu Graduate Research Innovation Program (grant no. XKYCX19\_153).

## REFERENCES

- (1) Hentze, M.; Schytte, S.; Pilegaard, H.; Klug, T. E. Single-stage tracheal and cricotracheal segmental resection with end-to-end anastomosis: Outcome, complications, and risk factors. *Larynx* **2019**, *46*, 122–128.
- (2) Krishnan, Y.; Grodzinsky, A. J. Cartilage diseases. *Matrix Biol.* **2018**, *71–72*, 51–69.
- (3) Etienne, H.; Fabre, D.; Caro, A. G.; Kolb, F.; Mussot, S.; Mercier, O.; Mitilian, D.; Stephan, F.; Fadel, E.; Dartevelle, P. Tracheal replacement. *Eur. Respir. J.* **2018**, *51*, 1702211.
- (4) Pfeiffer, M.; Cohn, J. E.; Pascasio, J. M.; Chennupati, S. K. Treatment of an obstructive, recurrent, syncytial myoepithelioma of the trachea with tracheal resection and reconstruction. *Int. J. Pediatr. Otorhinolaryngol.* **2018**, *109*, 85–88.
- (5) Wright, C.; Grillo, H.; Wain, J.; Wong, D.; Donahue, D.; Gaijssert, H.; Mathisen, D. Anastomotic complications after tracheal

resection: prognostic factors and management. *J. Thorac. Cardiovasc. Surg.* **2004**, *128*, 731–739.

(6) Sidell, D. R.; Hart, C. K.; Tabangin, M. E.; Bryant, R.; Rutter, M. J.; Manning, P. B.; Meinzen-Derr, J.; Balakrishnan, K.; Yang, C.; de Alarcon, A. Revision thoracic slide tracheoplasty: Outcomes following unsuccessful tracheal reconstruction. *Laryngoscope* **2018**, *128*, 2181–2186.

(7) Boazak, E. M.; Auguste, D. T. Trachea Mechanics for Tissue Engineering Design. *ACS Biomater. Sci. Eng.* **2018**, *4*, 1272–1284.

(8) Crowley, C.; Birchall, M.; Seifalian, A. M. Trachea transplantation: from laboratory to patient. *J. Tissue Eng. Regen. Med.* **2015**, *9*, 357–367.

(9) Weiss, D. J. Concise review: current status of stem cells and regenerative medicine in lung biology and diseases. *Stem Cell.* **2014**, *32*, 16–25.

(10) The, L. E. Expression of concern–Tracheobronchial transplantation with a stem-cell-seeded bioartificial nanocomposite: a proof-of-concept study. *Lancet* **2016**, *387*, 1359.

(11) Zhao, L.; Sundaram, S.; Le, A. V.; Huang, A. H.; Zhang, J.; Hatachi, G.; Beloiartsev, A.; Caty, M. G.; Yi, T.; Leiby, K.; et al. Engineered Tissue-Stent Biocomposites as Tracheal Replacements. *Tissue Eng., Part A* **2016**, *22*, 1086–1097.

(12) Atala, A.; Kasper, F. K.; Mikos, A. G. Engineering complex tissues. *Sci. Transl. Med.* **2012**, *4*, 160rv12.

(13) Ghorbani, F.; Moradi, L.; Shadmehr, M. B.; Bonakdar, S.; Droodnia, A.; Safshekan, F. In-vivo characterization of a 3D hybrid scaffold based on PCL/decellularized aorta for tracheal tissue engineering. *Mater. Sci. Eng., C* **2017**, *81*, 74–83.

(14) Orlando, G.; Wood, K. J.; Stratta, R. J.; Yoo, J. J.; Atala, A.; Soker, S. Regenerative medicine and organ transplantation: past, present, and future. *Transplantation* **2011**, *91*, 1310–1317.

(15) Hoshiba, T.; Lu, H.; Kawazoe, N.; Chen, G. Decellularized matrices for tissue engineering. *Exp. Opin. Biol. Ther.* **2010**, *10*, 1717–1728.

(16) Barrera Ramirez, E.; Garrido Cardona, R. E.; Rico Escobar, E.; Martinez Martinez, A.; Plenge Tellechea, L. F.; Hernandez, A.; Vanegas Venegas, E. Tissue engineering for regeneration in vivo of decellularized trachea scaffolds using a porcine model. *Eur. Respir. J.* **2018**, *52*, PA598.

(17) Baiguera, S.; Jungebluth, P.; Burns, A.; Mavilia, C.; Haag, J.; De Coppi, P.; Macchiarini, P. Tissue engineered human tracheas for in vivo implantation. *Biomaterials* **2010**, *31*, 8931–8938.

(18) Webber, A.; Hirose, R.; Vincenti, F. Novel strategies in immunosuppression: issues in perspective. *Transplantation* **2011**, *91*, 1057–1064.

(19) Gonfiotti, A.; Jaus, M. O.; Barale, D.; Baiguera, S.; Comin, C.; Lavorini, F.; Fontana, G.; Sibila, O.; Rombolà, G.; Jungebluth, P.; et al. The first tissue-engineered airway transplantation: 5-year follow-up results. *Lancet* **2014**, *383*, 238–244.

(20) Elliott, M. J.; De Coppi, P.; Speggorin, S.; Roebuck, D.; Butler, C. R.; Samuel, E.; Crowley, C.; McLaren, C.; Fierens, A.; Vondry, D.; et al. Stem-cell-based, tissue engineered tracheal replacement in a child: a 2-year follow-up study. *Lancet* **2012**, *380*, 994–1000.

(21) Maughan, E.; Lesage, F.; Butler, C. R.; Hynds, R. E.; Hewitt, R.; Janes, S. M.; Deprest, J. A.; Coppi, P. D. Airway tissue engineering for congenital laryngotracheal disease. *Semin. Pediatr. Surg.* **2016**, *25*, 186–190.

(22) van Veenendaal, M. B.; Liem, K. D.; Marres, H. A. M. Congenital absence of the trachea. *Eur. J. Pediatr.* **2000**, *159*, 8–13.

(23) Butler, C. R.; Hynds, R. E.; Crowley, C.; Gowers, K. H. C.; Partington, L.; Hamilton, N. J.; Carvalho, C.; Platé, M.; Samuel, E. R.; Burns, A. J.; et al. Vacuum-assisted decellularization: an accelerated protocol to generate tissue-engineered human tracheal scaffolds. *Biomaterials* **2017**, *124*, 95–105.

(24) Den Hondt, M.; Vanaudenaerde, B. M.; Maughan, E. F.; Butler, C. R.; Crowley, C.; Verbeken, E. K.; Verleden, S. E.; Vranckx, J. J. An optimized non-destructive protocol for testing mechanical properties in decellularized rabbit trachea. *Acta Biomater.* **2017**, *60*, 291–301.

- (25) Sun, F.; Pan, S.; Shi, H.-C.; Zhang, F.-B.; Zhang, W.-D.; Ye, G.; Liu, X.-C.; Zhang, S.-Q.; Zhong, C.-H.; Yuan, X.-L. Structural integrity, immunogenicity and biomechanical evaluation of rabbit decellularized tracheal matrix. *J. Biomed. Mater. Res., Part A* **2015**, *103*, 1509–1519.
- (26) Zang, M.; Zhang, Q.; Chang, E. I.; Mathur, A. B.; Yu, P. Decellularized Tracheal Matrix Scaffold for Tissue Engineering. *Plast. Reconstr. Surg.* **2012**, *130*, 532–540.
- (27) Parekkadan, B.; Milwid, J. M. Mesenchymal stem cells as therapeutics. *Annu. Rev. Biomed. Eng.* **2010**, *12*, 87–117.
- (28) Zhang, W.; Zhang, F.; Shi, H.; Tan, R.; Han, S.; Ye, G.; Pan, S.; Sun, F.; Liu, X. Comparisons of rabbit bone marrow mesenchymal stem cell isolation and culture methods in vitro. *PLoS One* **2014**, *9*, No. e88794.
- (29) Badylak, S. F.; Taylor, D.; Uygun, K. Whole-organ tissue engineering: decellularization and recellularization of three-dimensional matrix scaffolds. *Annu. Rev. Biomed. Eng.* **2011**, *13*, 27–53.
- (30) Parmaksiz, M.; Dogan, A.; Odabas, S.; Elçin, A. E.; Elçin, Y. M. Clinical applications of decellularized extracellular matrices for tissue engineering and regenerative medicine. *Biomed. Mater.* **2016**, *11*, 022003.
- (31) Crapo, P. M.; Gilbert, T. W.; Badylak, S. F. An overview of tissue and whole organ decellularization processes. *Biomaterials* **2011**, *32*, 3233–3243.
- (32) Bogan, S. L.; Teoh, G. Z.; Birchall, M. A. Tissue Engineered Airways: A Prospects Article. *J. Cell. Biochem.* **2016**, *117*, 1497–1505.
- (33) Zhong, Y.; Jiang, A.; Sun, F.; Xiao, Y.; Gu, Y.; Wu, L.; Zhang, Y.; Shi, H. A Comparative Study of the Effects of Different Decellularization Methods and Genipin-Cross-Linking on the Properties of Tracheal Matrices. *Tissue Eng. Regen. Med.* **2019**, *16*, 39–50.
- (34) Crapo, P. M.; Gilbert, T. W.; Badylak, S. F. An overview of tissue and whole organ decellularization processes. *Biomaterials* **2011**, *32*, 3233–3243.
- (35) Keane, T. J.; Londono, R.; Turner, N. J.; Badylak, S. F. Consequences of ineffective decellularization of biologic scaffolds on the host response. *Biomaterials* **2012**, *33*, 1771–1781.
- (36) Lange, P.; Greco, K.; Partington, L.; Carvalho, C.; Oliani, S.; Birchall, M. A.; Sibbons, P. D.; Lowdell, M. W.; Ansari, T. Pilot study of a novel vacuum-assisted method for decellularization of tracheae for clinical tissue engineering applications. *J. Tissue Eng. Regen. Med.* **2017**, *11*, 800–811.
- (37) Partington, L.; Mordan, N. J.; Mason, C.; Knowles, J. C.; Kim, H.-W.; Lowdell, M. W.; Birchall, M. A.; Wall, I. B. Biochemical changes caused by decellularization may compromise mechanical integrity of tracheal scaffolds. *Acta Biomater.* **2013**, *9*, 5251–5261.
- (38) Baiguera, S.; Del Gaudio, C.; Kuevda, E.; Gonfiotti, A.; Bianco, A.; Macchiarini, P. Dynamic decellularization and cross-linking of rat tracheal matrix. *Biomaterials* **2014**, *35*, 6344–6350.
- (39) Hussein, K. H.; Park, K.-M.; Kang, K.-S.; Woo, H.-M. Biocompatibility evaluation of tissue-engineered decellularized scaffolds for biomedical application. *Mater. Sci. Eng., C* **2016**, *67*, 766–778.
- (40) Berg, M.; Ejnell, H.; Kovács, A.; Nayakawde, N.; Patil, P. B.; Joshi, M.; Aziz, L.; Rådberg, G.; Hajizadeh, S.; Olausson, M.; et al. Replacement of a tracheal stenosis with a tissue-engineered human trachea using autologous stem cells: a case report. *Tissue Eng., Part A* **2014**, *20*, 389–397.
- (41) Jungebluth, P.; Alici, E.; Baiguera, S.; Blomberg, P.; Bozóky, B.; Crowley, C.; Einarsson, O.; Gudbjartsson, T.; Le Guyader, S.; Henriksson, G.; et al. Tracheobronchial transplantation with a stem-cell-seeded bioartificial nanocomposite: a proof-of-concept study. *Lancet* **2011**, *378*, 1997–2004.
- (42) Hamilton, N. J.; Kanani, M.; Roebuck, D. J.; Hewitt, R. J.; Cetto, R.; Culme-Seymour, E. J.; Toll, E.; Bates, A. J.; Comerford, A. P.; McLaren, C. A.; et al. Tissue-Engineered Tracheal Replacement in a Child: A 4-Year Follow-Up Study. *Am. J. Transplant.* **2015**, *15*, 2750–2757.
- (43) Weiss, D. J.; Elliott, M.; Jang, Q.; Poole, B.; Birchall, M. Tracheal bioengineering: the next steps. Proceeds of an International Society of Cell Therapy Pulmonary Cellular Therapy Signature Series Workshop, Paris, France, April 22, 2014. *Cytotherapy* **2014**, *16*, 1601–1613.
- (44) Fishman, J. M.; Wiles, K.; Lowdell, M. W.; De Coppi, P.; Elliott, M. J.; Atala, A.; Birchall, M. A. Airway tissue engineering: an update. *Expert Opin. Biol. Ther.* **2014**, *14*, 1477–1491.
- (45) Den Hondt, M.; Vanaudenaerde, B. M.; Verbeken, E. K.; Vranckx, J. J. Epithelial grafting of a decellularized whole-tracheal segment: an in vivo experimental model. *Interact. Cardiovasc. Thorac. Surg.* **2018**, *26*, 753–760.